ANNEX 4

TO

CHAPTER 2, PART II

Control Concept for the 30-m-Radiotelescope

TABLE OF CONTENT

ANNEX 4 TO CHAPTER 2, PART II
Control Concept for the 30-m-Radiotelescope

1. GENERAL

For operation of a 30 m radio telescope with which signals are to be received in millimeter wave range, an extremely high pointing and tracking accuracy must be ensured.

An antenna structure of sufficient rigidity and a drive control with exact functioning are absolutely necessary for this.

Linear mathematical spring-mass vibration models were prepared for dimensioning the mechanical structure which made it possible for natural frequencies to be obtained which were as high as possible and which were sufficiently far apart.

The same models could also be used as basis for simulations of controlled antenna movements.

First of all, conventional cascade control systems with additional setups for improving quality were investigated. This gave the result that the control quality could not meet the high demands, particularly under the influence of wind disturbance.

New paths therefore had to be opened up to reach distinct improvements of the control response.

Thus for the first time for antenna controls, a procedure of modern control theory; controller design in state space with the aid of pole assignment, which has only been developed in recent years, was applied and examined by extensive simulation tests.

A significant improvement of the dynamic performance was apparent as compared with classical cascade control.

Both control concepts are described in more detail below and are compared. The essential characteristics of the mathematic antenna simulation however are described initially.

Only the elevation control is considered here; the azimuth control is of similar setup.

2. ANTENNA SIMULATION EL

The basic setup of the 30 m radio telescope is shown in Fig. 2/1.

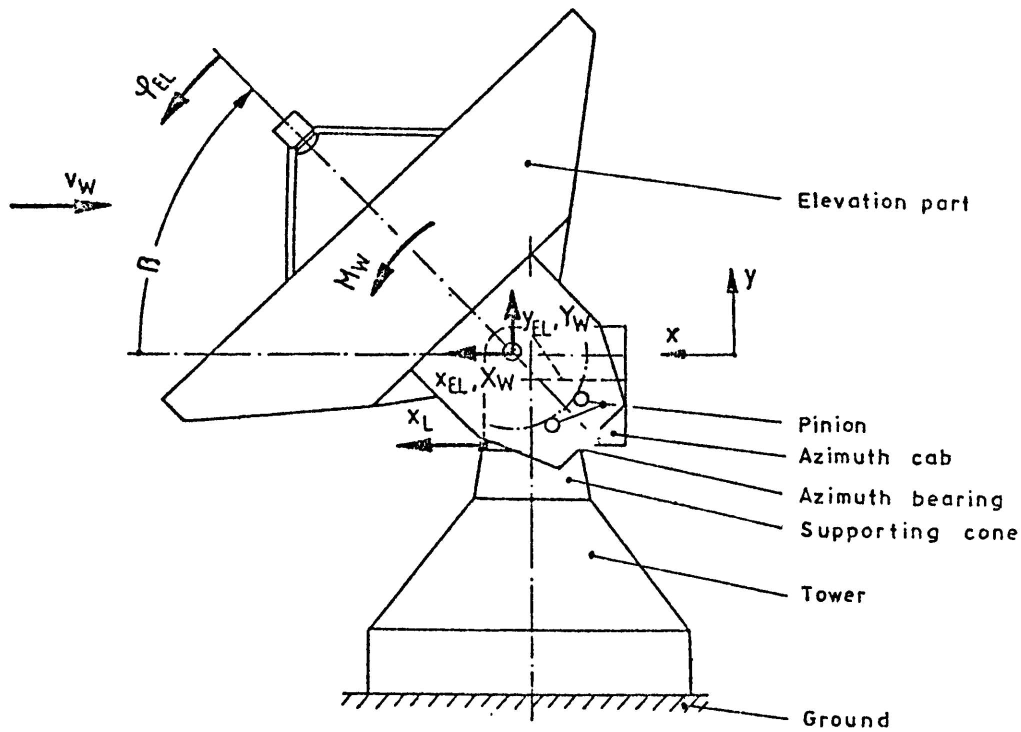

Fig. 2/1 Assembly Groups of the 30 m Radio Telescope

An antenna of this size cannot be designed with just any rigidity. Unwanted effects occur which limit pointing accuracy. The following must be particularly considered here:

- elevation and azimuth bearings are resilient;
- tower and supporting cone are not rigid, they bend;
- considering the great weight of the tower, and moments occurring in the tower anchoring due to wind disturbance, the elasticity of the ground must not be neglected;
- there is no proportional relation between motor speed and pinion speed as a result of torsional load.

In order to be able to analyse these influences, a mechanical spring-mass model was first of all developed which contains all elasticities and masses responsible for the important low-frequency oscillation.
The mathematical model of the antenna in the form of a differential equation system was obtained from this with the aid of the method of virtual displacements and mathematical transformations for reducing the number of movement influences.

The state-space representation usual in modern control technology proved to be a particularly favourable system description

$$\dot{\underline{x}}(t) = \underline{A}\,\underline{x}\,(t) + \underline{b}\,u(t) + \underline{B}_Z\,\underline{z}(t) + \underline{f}\,(\underline{x}) \qquad (2/1)$$

with the time-dependent state vector:

$$\underline{x}(t) = (x_{EL},\, y_{EL},\, \varphi_{EL},\, \varphi_M,\, x_L,\, \dot{x}_{EL},\, \dot{y}_{EL},\, \dot{\varphi}_{EL},\, \dot{\varphi}_M,\, \dot{x}_L)^T, \qquad (2/2)$$

which includes the following movement influences and their time derivatives (speeds):

x_{EL} = shifting of elevation part in x direction,

y_{EL} = shifting of elevation part in y direction,

φ_{EL} = turning of elevation part,

φ_M = rotation of motor shaft,

x_L = shifting of azimuth bearing in x direction.

The resulting moment of all motors M_M with parallel effect is applied as control influence:

$$u\,(t) = M_M(t). \qquad (2/3)$$

The disturbance vector

$$\underline{z} = (x_W, y_W, M_W)^T \qquad (2/4)$$

includes the wind forces acting on the elevation axis in horizontal and vertical direction x_W and y_W respectively as well as the wind moment M_W.

$\underline{A}$ is the (10 x 10) system matrix which contains all information on the system - thus structure and parameter.

$\underline{b}$ is the (10 x 1) control vector, $\underline{B}_Z$ the (10 x 3) disturbance matrix.

A non-linear (10 x 1) friction term $\underline{f}$ $(\underline{x})$ which takes gear frictions into account can be added.

From

$$\det (s\underline{I} - \underline{A}) = \underline{0} \qquad (2/5)$$

the eigen values (≡ poles) of the system are obtained. They are applied in Fig. 2/2 in the complex s-plane.

The natural frequencies $f_i = \omega_{j,k}/2\pi$ result from this:

f_1 = 0,000 Hz,
f_2 = 3,845 Hz,
f_3 = 7,558 Hz,
f_4 = 24,100 Hz,
f_5 = 77,280 Hz.

The double pole which is part of frequency f_1, and which indicates unstable double-I behaviour, is due to the free rotatability of the motors which are not blocked by the brakes. The poles varying from zero distinguish the undamped oscillating behaviour as long as no inner or external damping is effected.

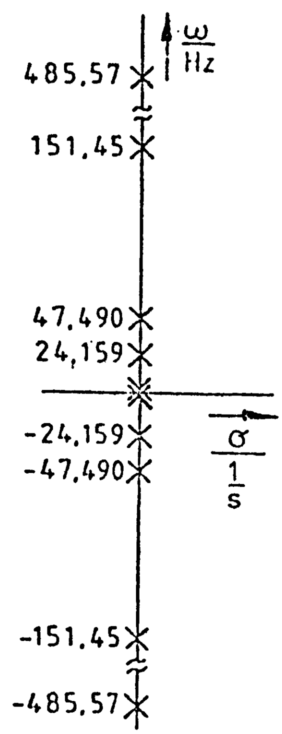

Fig. 2/2
Pole distribution in the complex s-plane

These results are confirmed by appropriate simulations of the system which is still not controlled.
The oscillating behaviour assessed with the analogous computer of all state variables at a wind gust speed of 0 to 14 m/s, and unfavourable reflector position, is applied in figs. 2/3 and 2/4.

The simulation result more or less clearly confirms the natural frequencies.

It is particularly noticeable that the reflector and the motor shafts coupled by the gearings are turned away by wind force, i.e. indicate the double-I characteristic already mentioned.

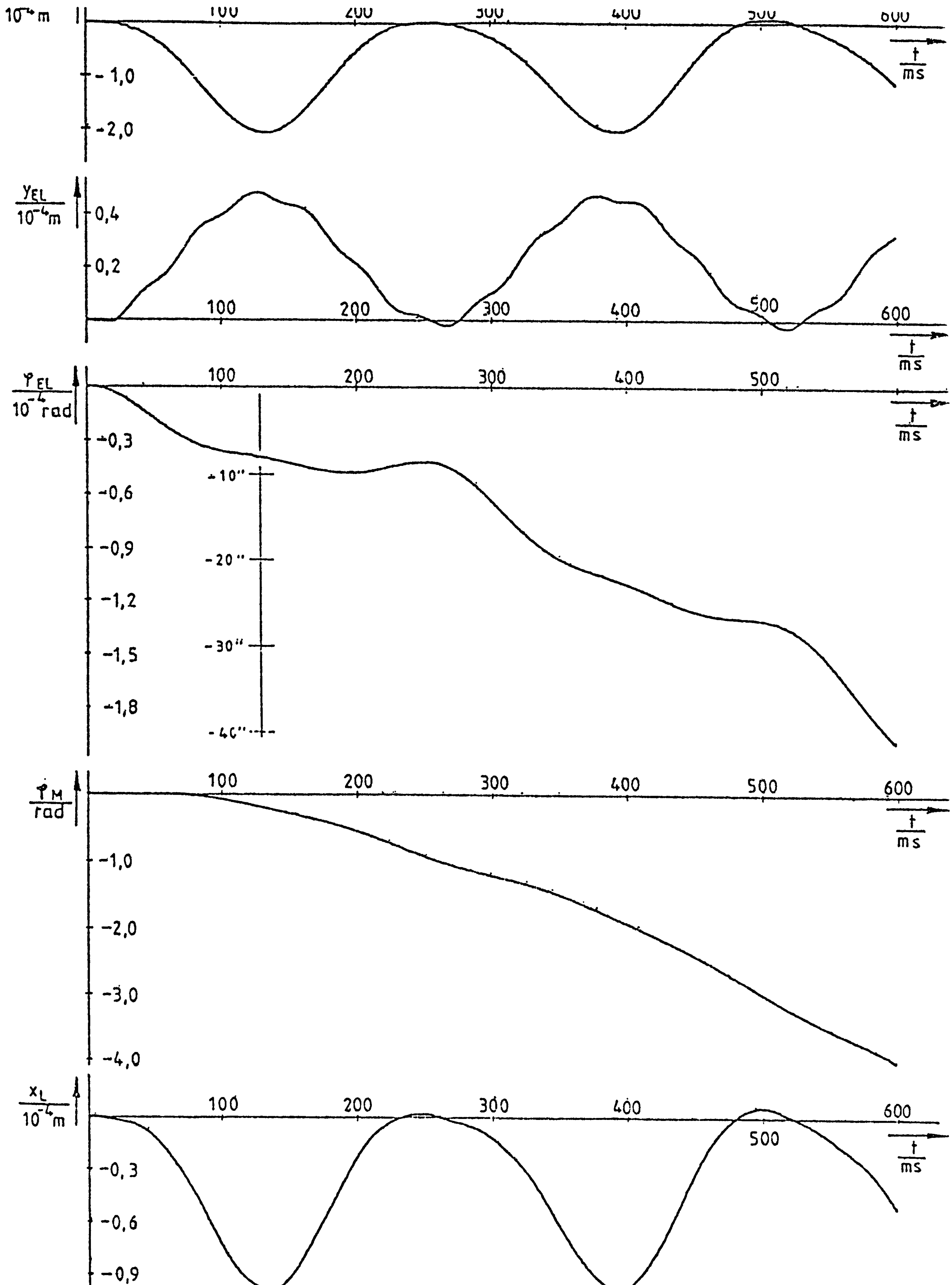

Fig. 2/3 Disturbance Response of the State Variables for a Wind Step 0-14 m/

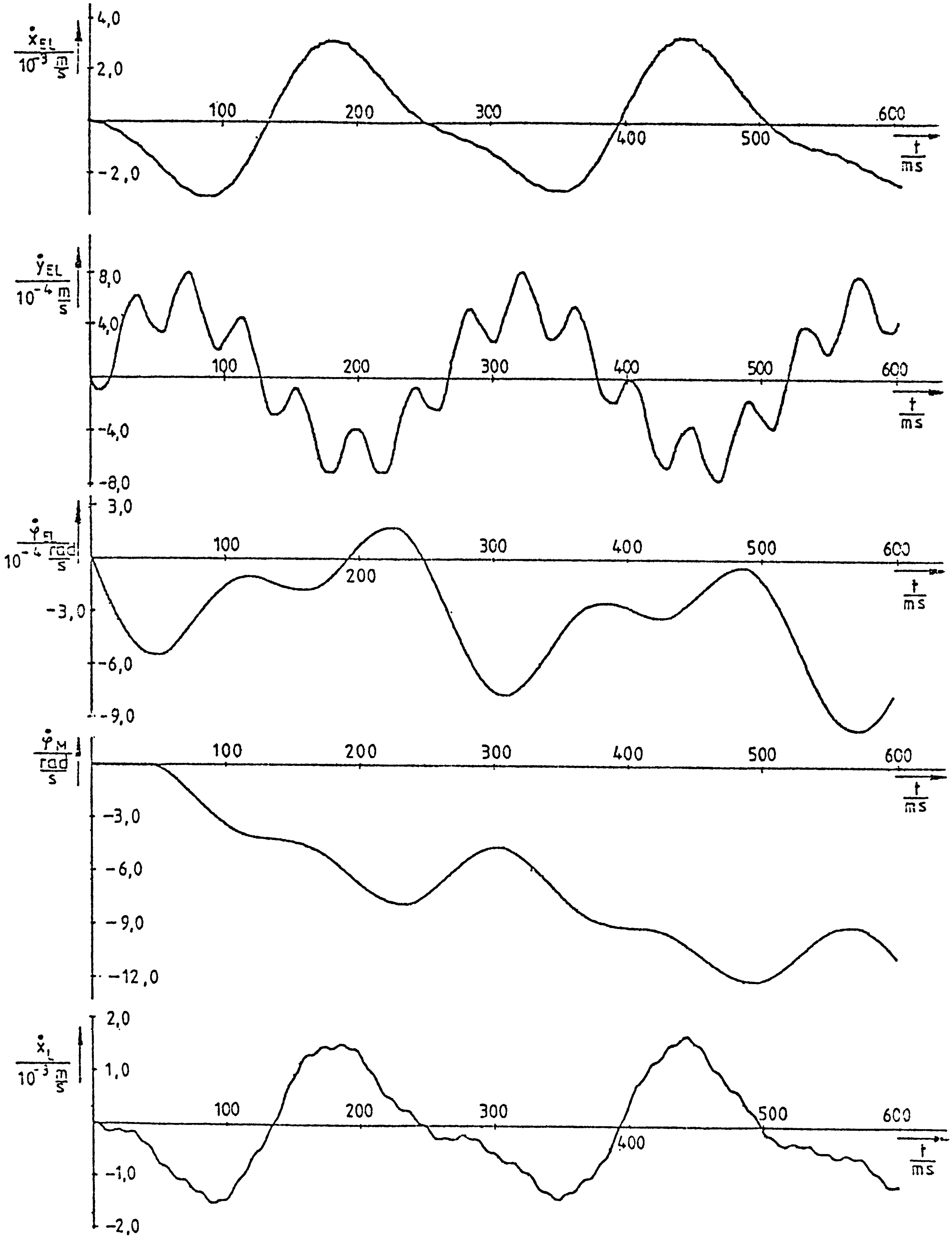

Fig. 2/4 Disturbance Response of the State Variables for a Wind Step 0-14 m/s

3. CONTROL CONCEPTS

Before the control concepts can be described, several remarks on the measuring system are necessary.

3.1 MEASURING SYSTEM

Various measurements of the system movements are necessary to permit a statement to be made on the momentary condition of the controlled system, and also to realize the influencing factors for the controllers introduced in the following chapters. Not all movements are accessible for measurement in practice.

The most important measured value is the elevation angle φ_{EL} characterizing the direction of observation. An incremental angle encoder is used for determining this, which is rigidly coupled to the azimuth cab. The required measurement of φ_{EL} is therefore invalidated by the inclination of the azimuth cab, so that the encoder indicates the value

$$\varphi^*_{EL} = \varphi_{EL} + \varphi_H. \qquad (3.1/1)$$

As the tests of the control systems (see chapter 3.2) indicate, the measurement of φ_H cannot be dispensed with. For this purpose, an inclination measurement device is used which records wandering of the azimuth cab away from horizontal, with the necessary dynamics.

The motor speeds $\dot{\varphi}_M$ are determined using tacho generators.

For the state controller (see chapter 3.3), the positions of the motor shafts are also measured with incremental encoders.

3.2 CASCADE CONTROL

Controller

Fig. 3.2/1 shows the basic structure of a cascade control system which can be used for flexible drives.

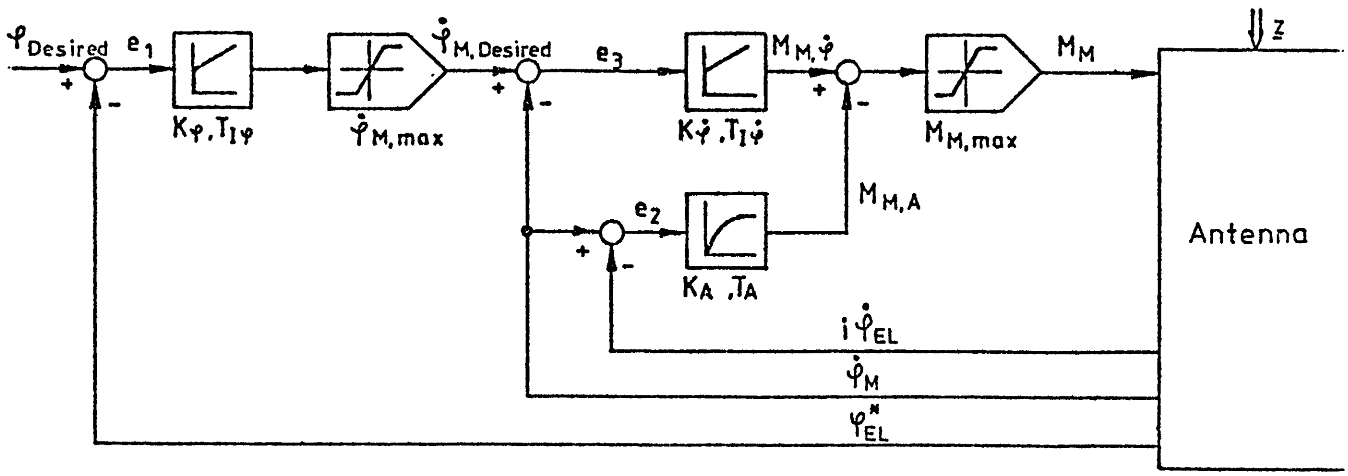

Fig. 3.2/1 Cascade Controller

It is to be considered here that, with a view to simplifying the simulations, the individual motor moments have been joined to form a total moment.

The controller is composed of a position controller and a speed controller which are connected in line one behind the other to form a cascade. Both controllers have a PI structure.
The input variables of the position and speed controllers are the control deviations of the elevation angle

$$e_1 = \varphi_{Desired} - \varphi^*_{EL} \tag{3.2/1}$$

or the motor speed

$$e_3 = \dot{\varphi}_{M,Desired} - \dot{\varphi}_M, \tag{3.2/2}$$

whose nominal value is given as output variable of the position controller.

In order to consider the influence of the different oscillations between the motors and the elevation part during control, practice has proved that a PT_1 link should be negatively setup. The difference between motor speed and the elevation speed at motor shaft (i = total transmission)

$$e_2 = \dot{\varphi}_M - i\dot{\varphi}_{EL} \tag{3.2/3}$$

on the input of the delay element is given as measure for these oscillations. Thus, the motor moment

$$M_M = M_{M,\dot{\varphi}} - M_{M,A} \tag{3.2/4}$$

is diminished so that less over-swinging of the elevation angle φ_{EL} can be expected.

The physical limitations of motor speed and motor moment are indicated by the limiters $\dot{\varphi}_{M,max}$ and $M_{M,max}$ in the circuit diagram. The entire controller is described by the equations (3.2/1...4) and the following relationships:

$$\dot{\varphi}_{M,Desired} = K_\varphi \left[e_1(t) + \frac{1}{T_{I\varphi}} \int_0^t e_1(\tau)\, d\tau\right], \tag{3.2/5}$$

$$M_{M,\dot{\varphi}} = K_{\dot{\varphi}} \left[e_3(t) + \frac{1}{T_{I\dot{\varphi}}} \int_0^t e_3(\tau)\, d\tau\right], \tag{3.2/6}$$

$$M_{M,A} = \frac{1}{T_A} \int_0^t \left[K_A\, e_2(\tau) - M_{M,A}(\tau)\right] d\tau. \tag{3.2/7}$$

Simulation Results

All simulations were carried out for an elevation angle of 80°, since the wind disturbance moment assumes maximum amount at this position.

Fig. 3.2/2 shows the antenna disturbance with a wind gust speed 0 to 14 m/s., assumed as test signal. A constant deviation of about 2" is clearly apparent between the encoder measured quantity φ^*_{EL} and the absolute elevation angle φ_{EL}.

As already indicated in chapter 3.1, the error results from inclination φ_H of the azimuth cab.
In order to avoid this error, the measurement of φ_H must be included without fail in the measuring system.

Further essential information on the reaction of the controlled antenna can be seen in the amplitude characteristic. Fig. 3.2/3 shows the system response on sinusoidal disturbances of various frequencies, but of uniform amplitudes. The high natural frequencies of the non-controlled system are significantly reduced by the controller. This has the decisive disadvantage in that stimulation of the control circuit is possible due to low-frequency disturbances.

Fig. 3.2/4 and 3.2/5 include the guide ramp response for adjustment (300"/sec.) and measurement (1"/sec.). No constant control deviations occur - other than for wind disturbances.

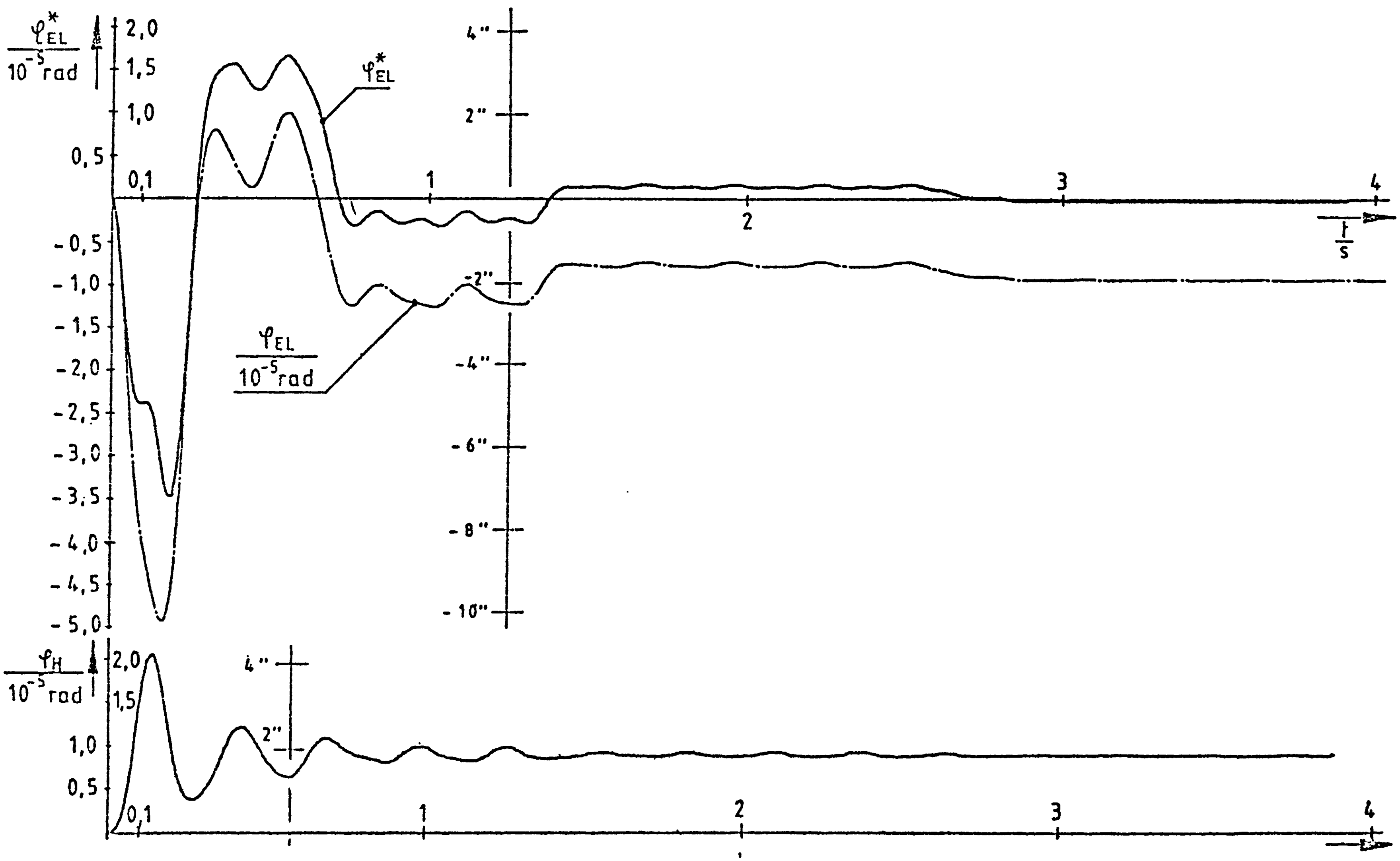

Fig. 3.2/2 Disturbance Response for a Wind Step 0-14 m/s; Cascade Controller

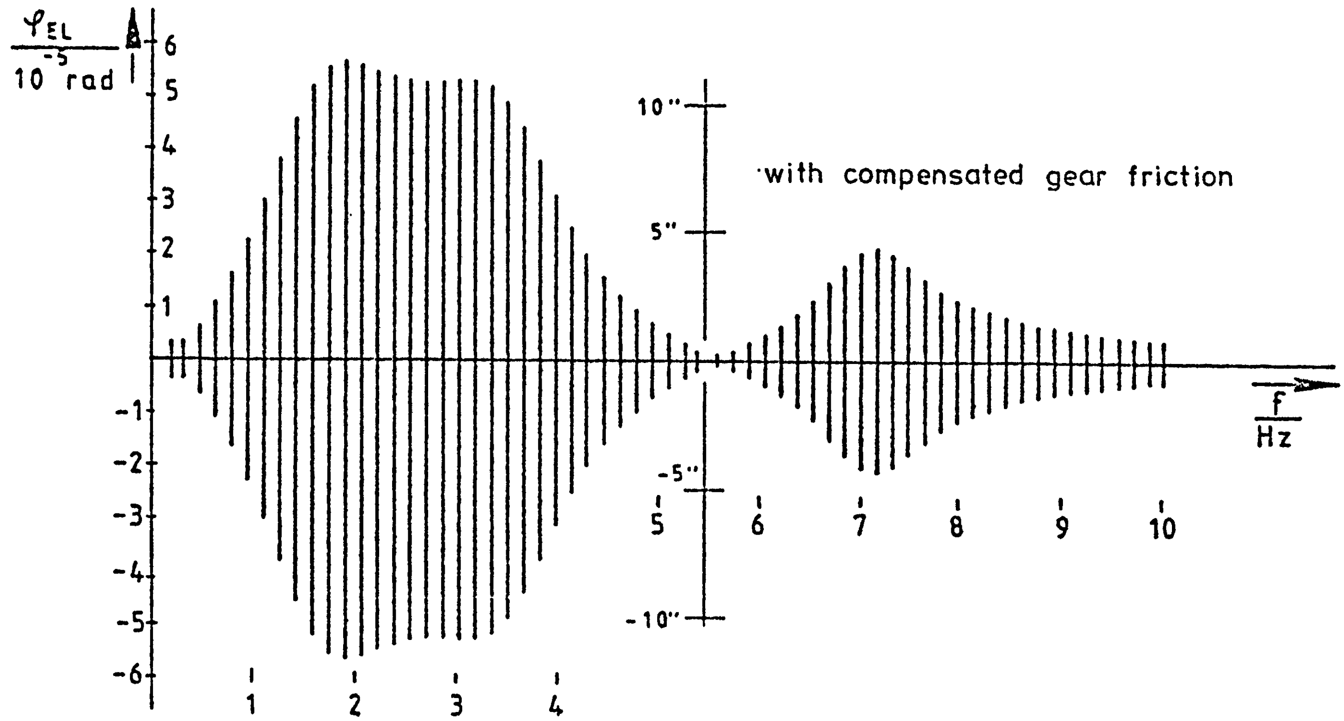

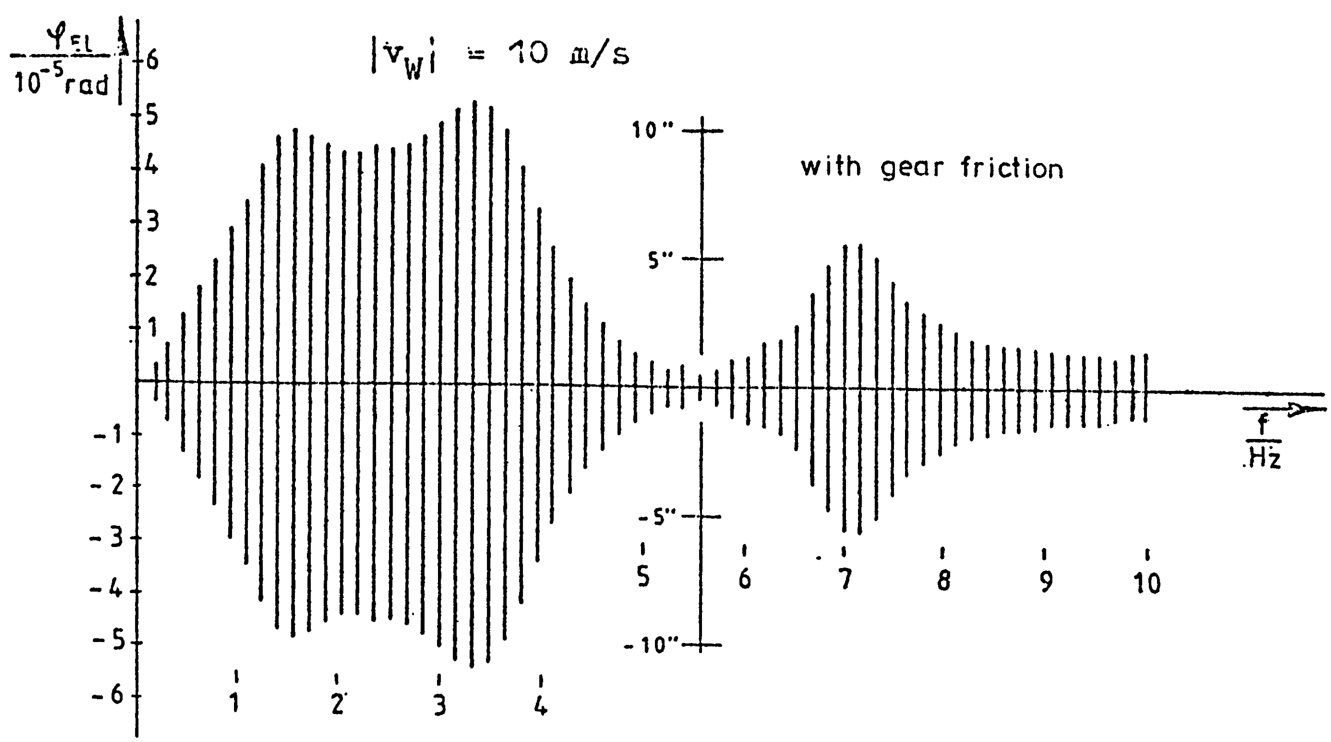

Fig. 3.2/3 Amplitude Response for sine-shaped Wind Disturbance, Cascade Controller

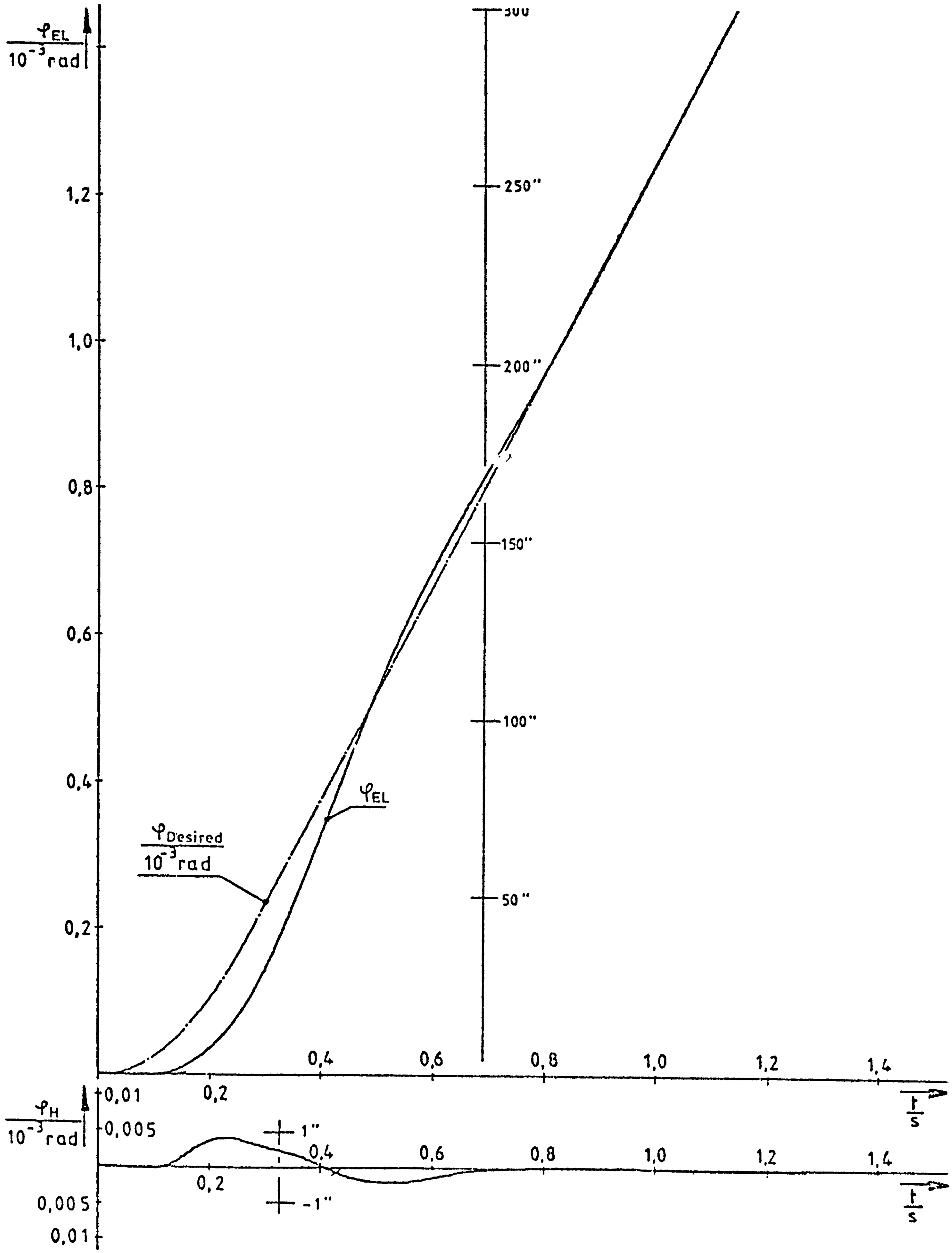

Fig. 3.2/4 Guide Ramp Response for a Ramp 300"/s, Cascade Controller

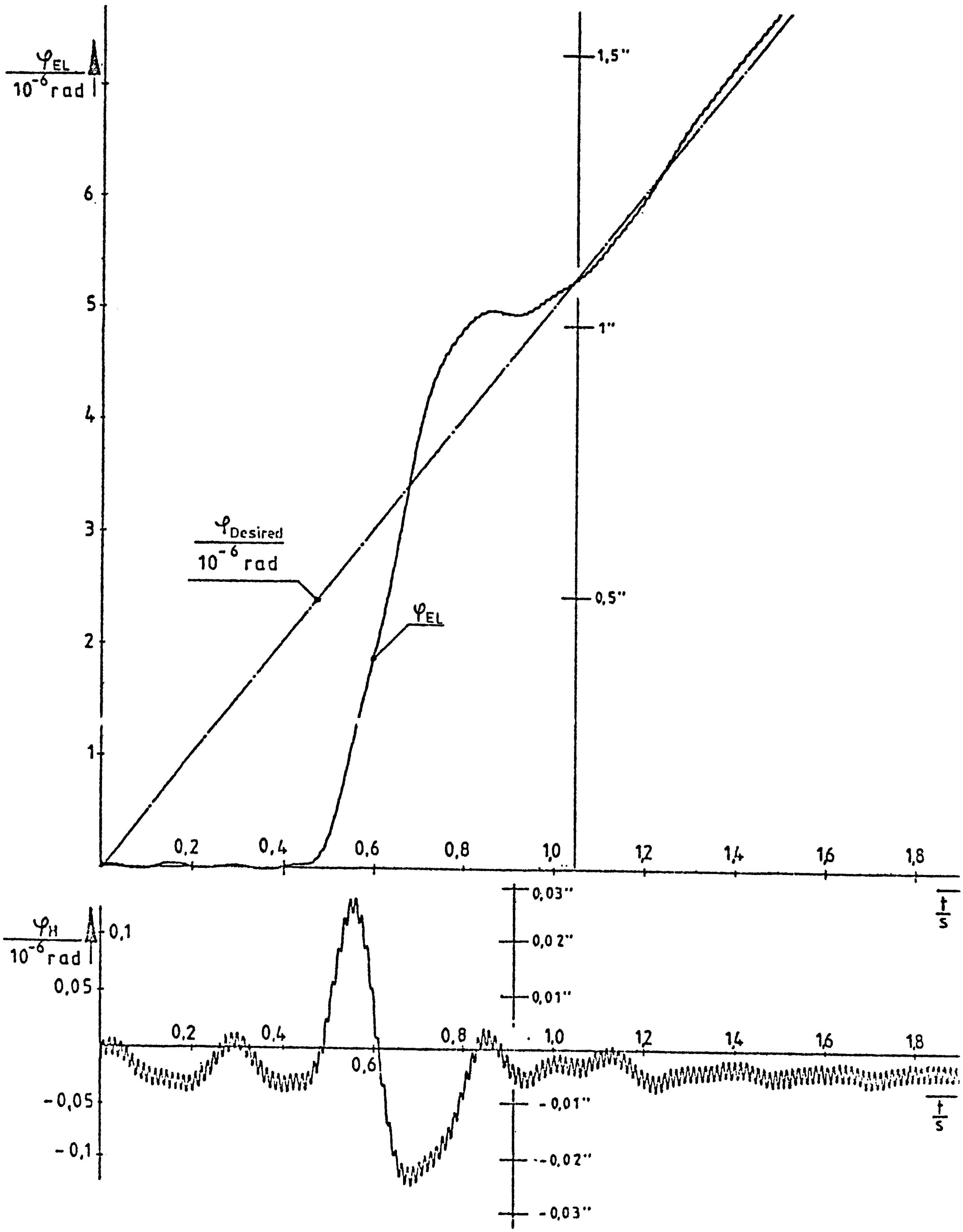

Fig. 3.2/5 Guide Ramp Response for a Ramp 1"/s, Cascade Controller

3.3 STATE CONTROL

With the cascade control concept, satisfactory characteristics are obtained for the case, important in practice, of a ramp guide signal, but step and sinusoidal wind disturbances are only inadequately stabilized. The limited control quality is due to the controller not being provided with sufficient information on kinetic quantities of the antenna. This inadequacy does not affect the state controller described below.

State Controller
With the cascade controller, the optimization of the closed circuit leads to a reduction of the natural frequencies (see chapter 3.2) with all the disadvantages arising from this.

The particular advantage of the state controller is the possibility of being in a position to determine exactly all the system eigen values in their frequency as well as in their damping. The natural frequencies can therefore be set so high that low frequency disturbances can hardly influence the system. In addition, by suitable selection of the controller structure for certain classes of disturbance and guide signals, constant control deviations can be prevented.

Fig. 3.3/1 shows the basic structure of the state control system for the 30-m radio telescope.

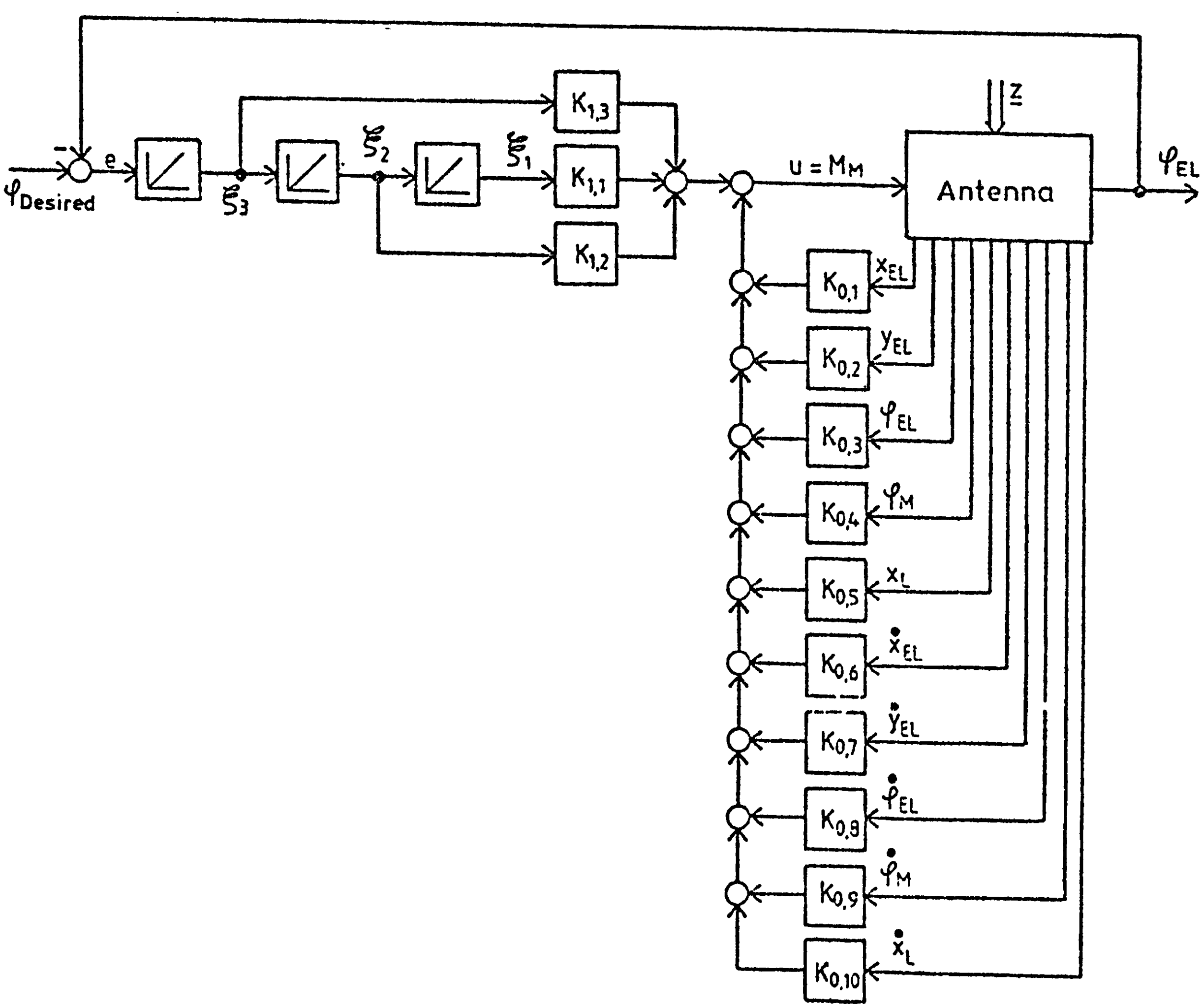

Fig. 3.1/1 Block diagram for state control of elevation movement

The three integrators which further integrate the controller deviation

$$e = \varphi_{Desired} - \varphi_{EL} \qquad (3.3/1)$$

have the effect that no constant control deviations occur for the following guide and disturbance signals;
step, ramp and parabola.
The parabola is of particular importance here since signals changing sinusoidally can be described in initial approximation due to parabolic branches.

All states of the antenna (see chapter 2) are led back in the same way as the controller states ξ_1, ξ_2, ξ_3, via proportional links:-

$$M_M = (K_{01}, K_{02}, \dots, K_{0.10})\, \underline{X} + (K_{1.1}, K_{1.2}, K_{1.3})\, \underline{\xi},$$

$$\underline{\xi} = (\xi_1, \xi_2, \xi_3)^T. \qquad (3.3/2)$$

The system dynamic is determined with the aid of these proportional links

The controller parameters $K_{i,j}$ necessary for any distribution of the eigen values (pole assignment) can be determined by extensive matrix calculations by computer.
Excellent control results for example have been obtained with dominating natural frequences of 5 Hertz and 10 Hertz. A comparison of these frequencies with the natural frequencies of the non-controlled system (see chapter 2) indicates that the values can even be increased (!) - as clearly opposed to the cascade control.

A disadvantage of the state controller introduced here is the great amount of hardware required, as a result of the necessity of measuring all antenna states.

Particular efforts were therefore made to simplify the controller - keeping the excellent control characteristics.

Fig. 3.3/1 shows the control structure resulting from these demands.

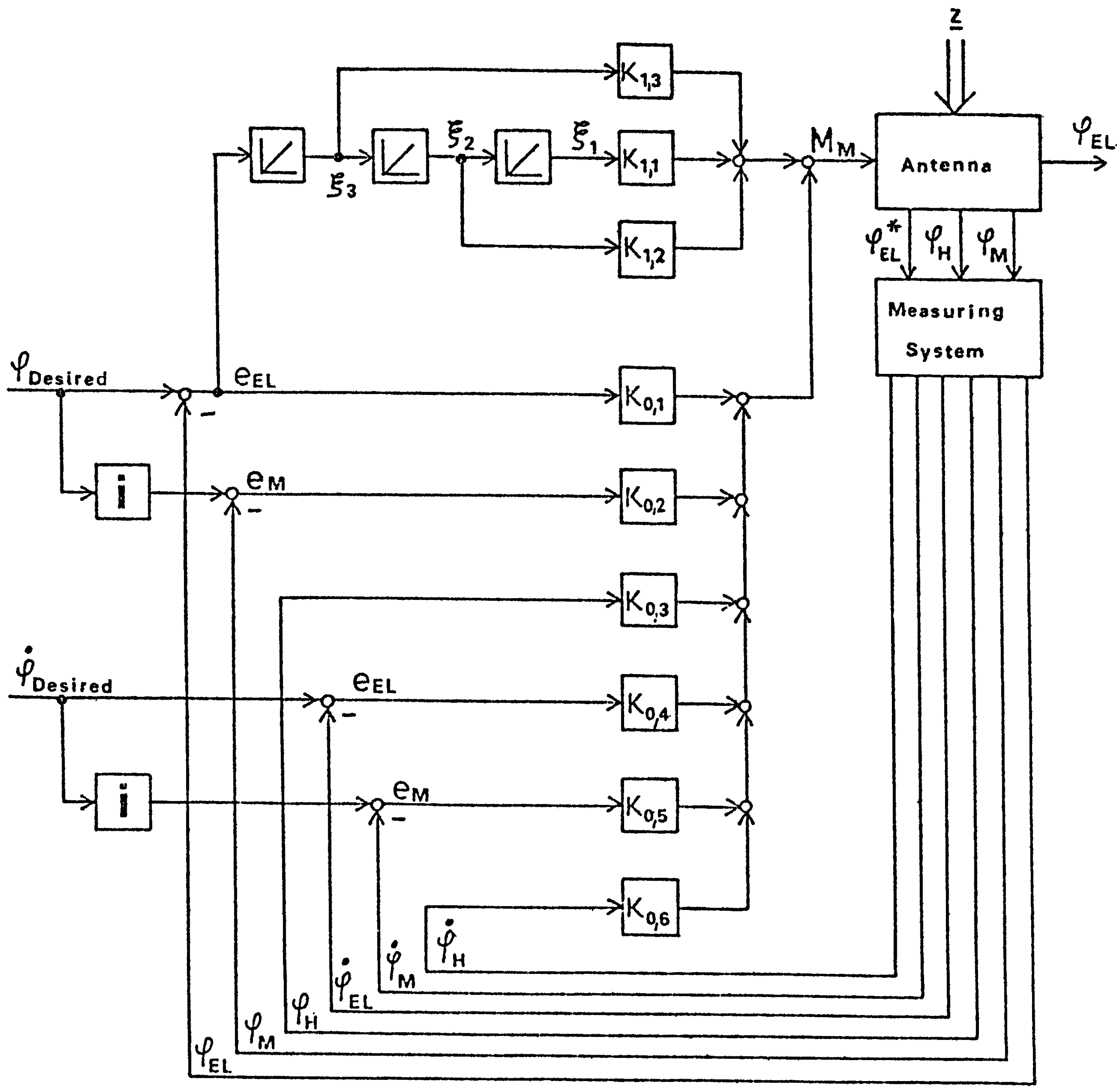

Fig. 3.3/2 Simplified state controller

The number of restoring states could be reduced from an original ten to six.
It suffices when the following antenna movements are measured:

- angle between elevation axis and azimuth cab φ^*_{EL},
- inclination of azimuth cab φ_H,
- mean value of motor shaft positions φ_M.

The missing quantities are formed electronically from those measured.

The nominal/actual value comparisons for positions

$$e_{EL} = \varphi_{Desired} - \varphi_{EL} \qquad (3.3/3a)$$

$$e_M = i\varphi_{Desired} - \varphi_M \qquad (3.3/3b)$$

and the relevant speeds

$$\dot{e}_{EL} = \dot{\varphi}_{Desired} - \dot{\varphi}_{EL} \qquad (3.3/3c)$$

$$e_M = i\dot{\varphi}_{Desired} - \dot{\varphi}_M \qquad (3.3/3d)$$

have the advantage that the computer is not burdened with very high figures when carrying out the control algorithm - as opposed to controller as per fig. 3.3/1.

Simulation Results

Fig. 3.3/3 shows a direct comparison of the disturbance responses of the elevation angle φ_{EL} to a wind gust speed of 0 to 12 m/s, with the state and cascade control. Apart from a less depth of penetration, the state controller is distinguished by a much shorter stabilizing time.

A further essential advantage is the very favourable disturbance amplitude characteristic as per fig. 3.3/4. Hardly any activation worth mentioning occurs up to frequencies of about 3.5 Hertz. An additional improvement is possible with electric compensation of the gearing static friction.

Since a wind changing in steps never occurs in nature, investigations were made as to how a slight wind force influences the control response. Curves às per fig. 3.3/5, lower left-hand side, have been assumend for the wind forces on the elevation bearing in horizontal direction X_W or in vertical direction Y_W and wind moment M_W. The disturbance responses indicated in the same figure, depending on the delay time T_a, clarify the positive influence of the high natural frequencies; even from T_a = 0.3 seconds, the antenna hardly travels out.

Examples for the guide behaviour are shown in figs. 3.3/6 and 3.3/7. The control deviation e_{EL} has been included to elucidate the control quality.

All simulations have been based on the quasi-continuous measurement of the elevation angle.

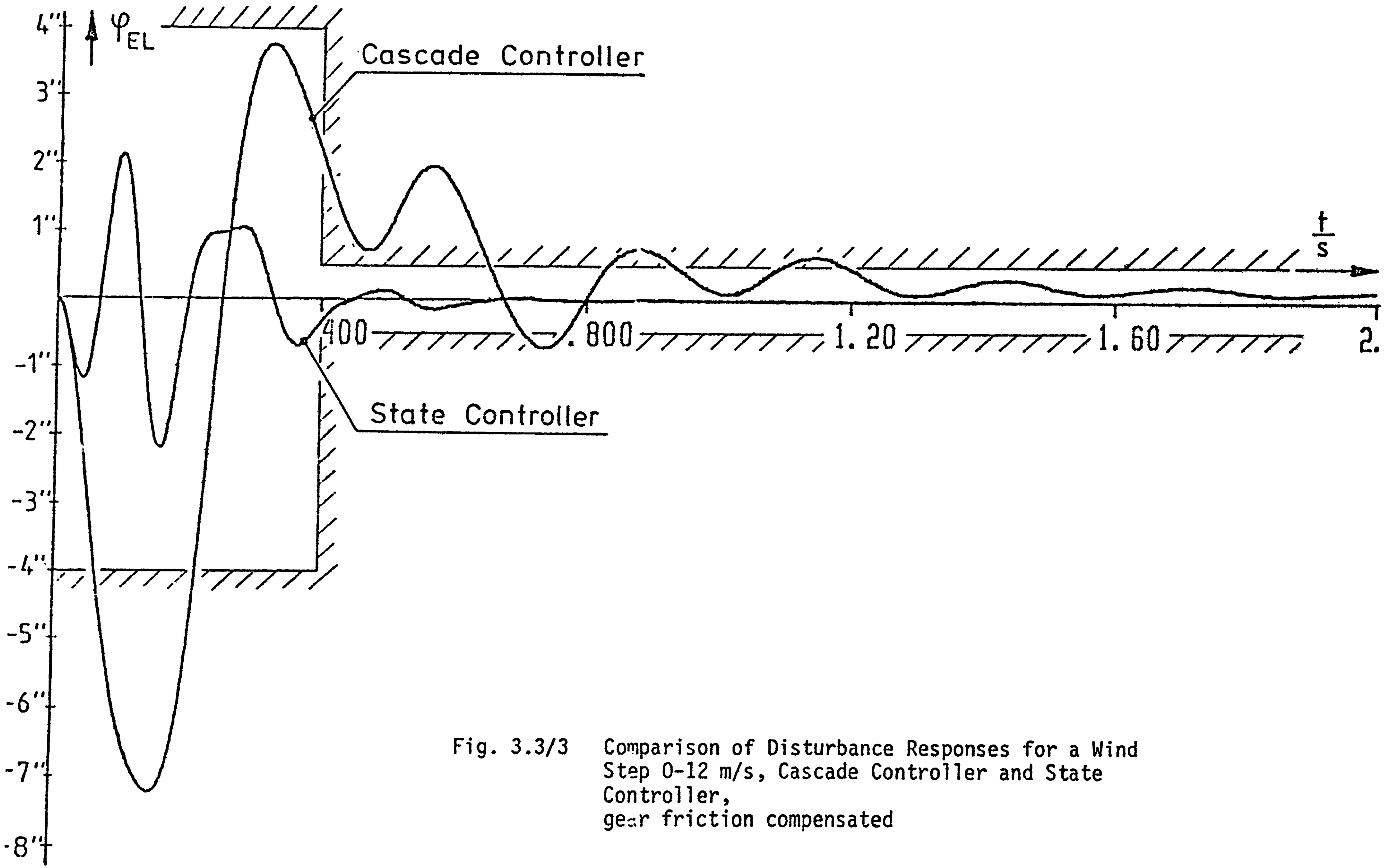

Fig. 3.3/3 Comparison of Disturbance Responses for a Wind Step 0-12 m/s, Cascade Controller and State Controller, gear friction compensated

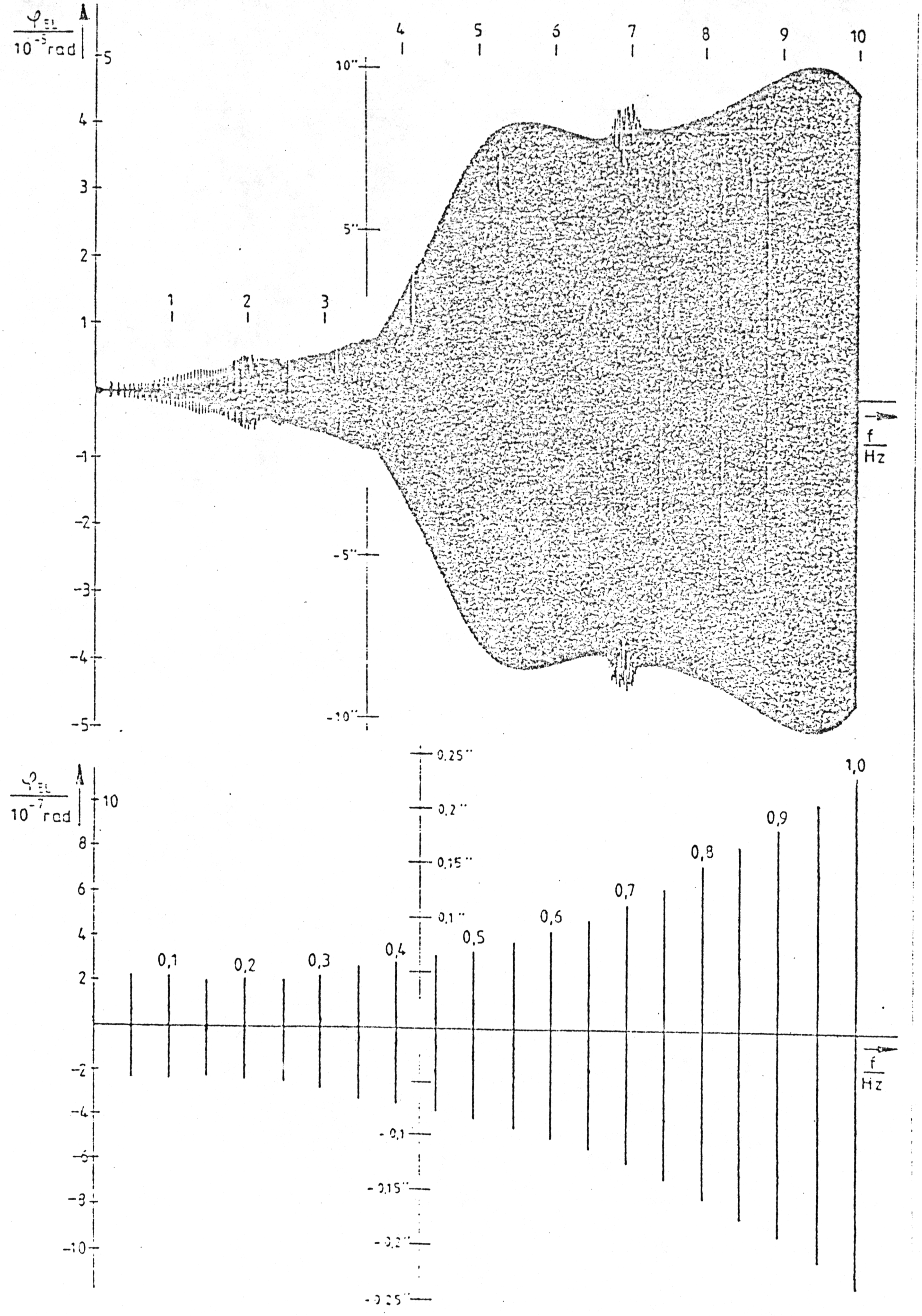

Fig. 3.3/4 Amplitude Response for a sine-shaped Wind Disturbance $V_W = \pm 12$ m/s, with gear Friction, State Controller

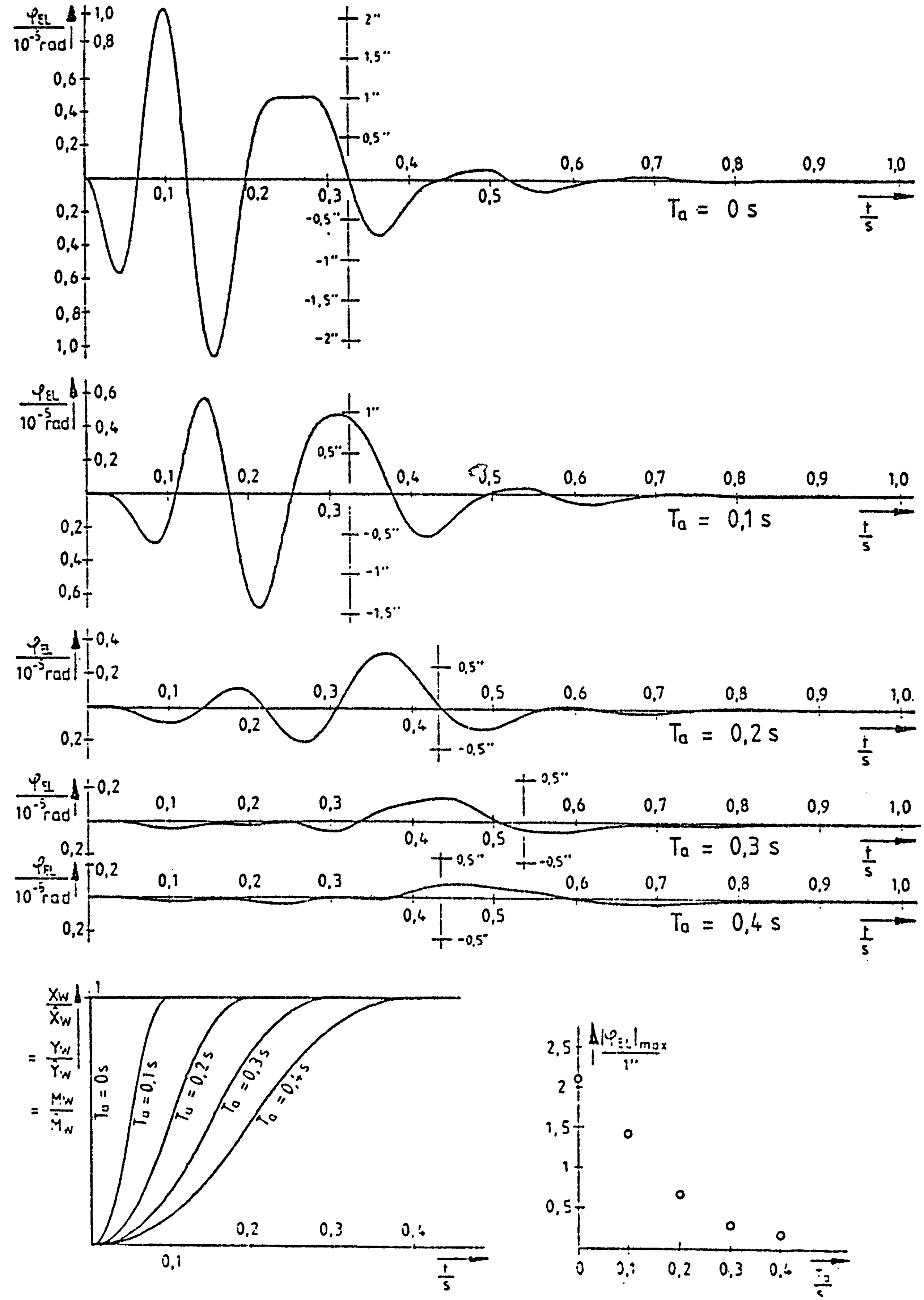

Fig. 3.3/5 Disturbance Response for a delayed Wind Step 0-12 m/s, State Controller

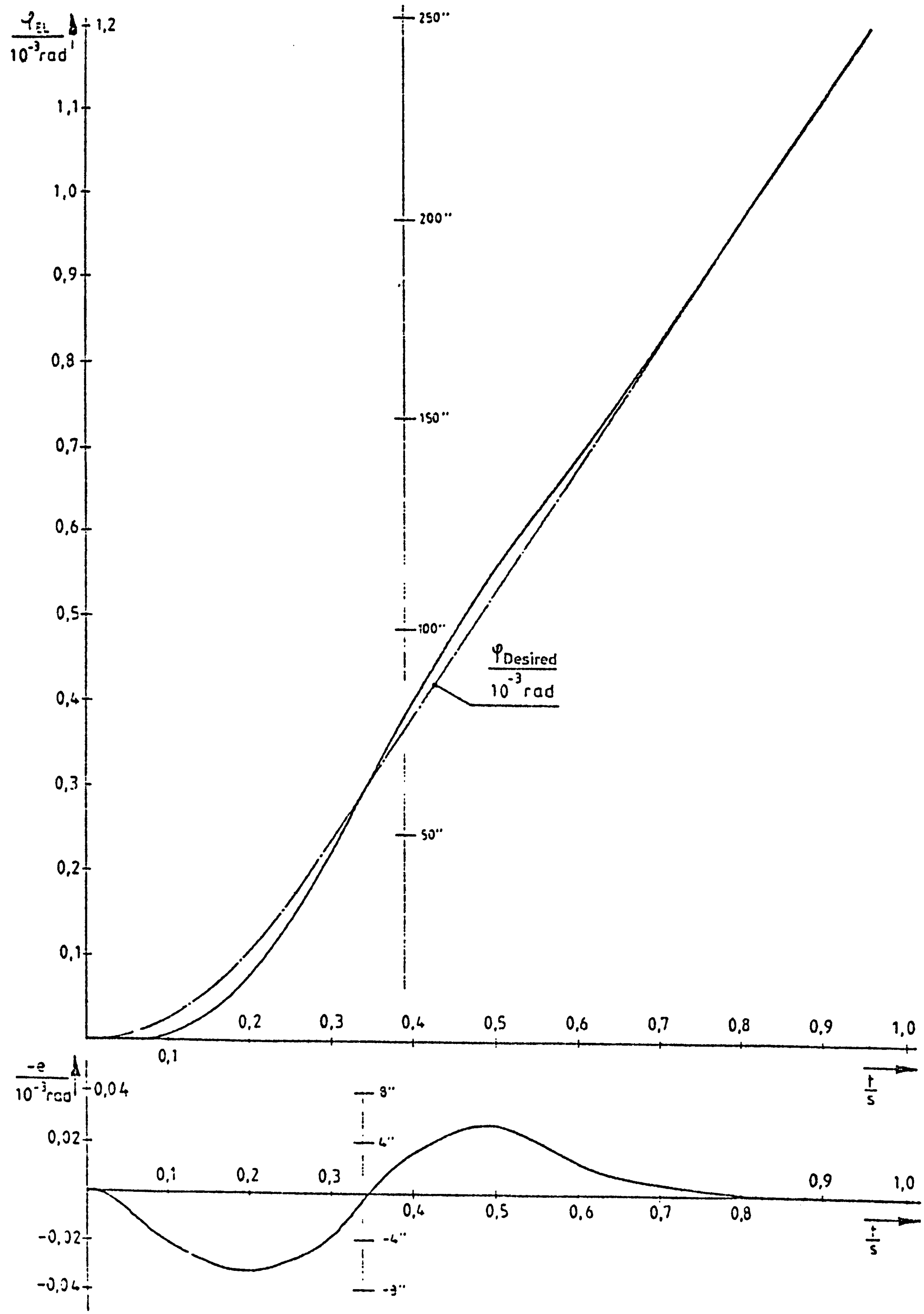

Fig. 3.3/6 Guide Ramp Response for a Ramp 300"/s, State Controller

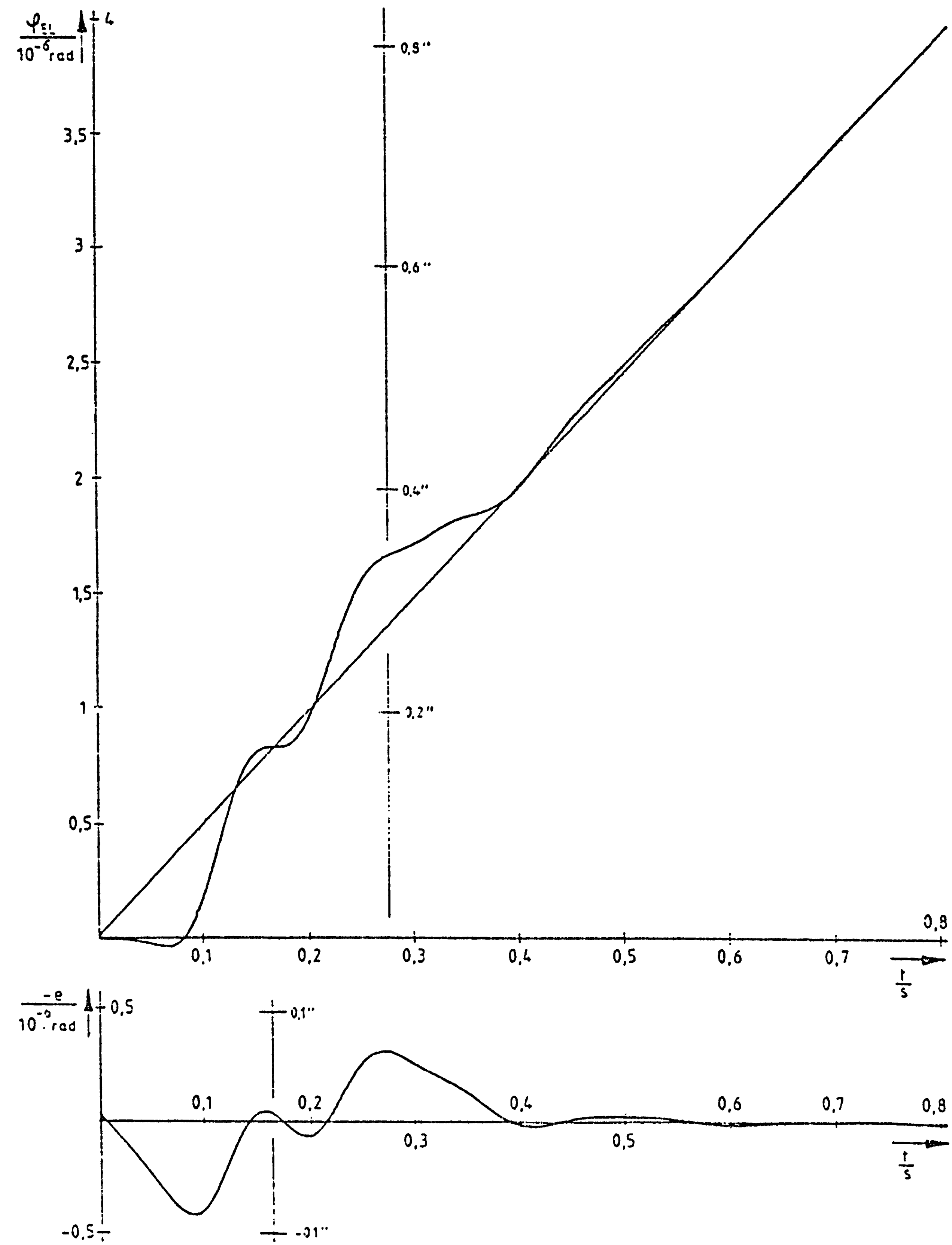

Fig. 3.3/7 Guide Ramp Response for a Ramp 1"/s,
State Controller

3.4 ADDITIONAL SUPERIMPOSED CONTROL SYSTEMS

Apart from the main control circuit described so far, additional control circuits are installed for preventing oscillation between the two backlash motors of one drive unit, and between the drives of the two elevation halves (compare chapter 2.2.3.4 of the technical proposal).

Power control circuits can be added, which can be neglected as a result of their low time constants for the simulations.

4. SUMARY

This description of control concepts for the 30-m radio telescope primarily handles a conventional cascade control on the basis of a mathematic antenna simulation. The controller structure and obtainable control results were investigated.
A modern state control was then introduced with its main characteristics.
Finally, additional superimposed control circuits were briefly mentioned.

A comparison between cascade and state control indicates - for guide as well as for disturbance behaviour - a significant superiority of the state controller, which indeed has to be bought with its higher amount of hardware and software.